

In situ neutron diffraction study of the behaviour of $\text{LaNi}_{4.5}\text{Al}_{0.5}\text{D}_x$ electrode during deuterium charge–discharge

M. Latroche and A. Percheron-Guegan

Laboratoire de Chimie Métallurgique des Terres Rares, CNRS, 1 Place A. Briand, 92195 Meudon Cedex (France)

Y. Chabre

Laboratoire de Spectrométrie Physique, Université J. Fourier–Grenoble I, BP87, 38402 Saint Martin d'Hères (France)

C. Poinignon

L.I.E.S.G.–E.N.S.E.E.G., I.N.P. Grenoble, BP 75, 38402 Saint Martin d'Hères (France)

J. Pannetier

Institut Laue Langevin, 156X, 38042 Grenoble (France)

(Received February 10, 1992; in final form April 7, 1992)

Abstract

The behaviour of $\text{LaNi}_{4.5}\text{Al}_{0.5}\text{D}_x$ was studied by *in situ* neutron powder diffraction during an electrochemical deuterium charge–discharge cycle. The phases involved in the transformation were identified and the evolution of their cell parameters during the charge–discharge reaction was analysed. Phases with out-of-equilibrium cell parameters are observed related to the charge–discharge rate.

1. Introduction

Intermetallic hydrides with high hydrogen concentration are good candidates for the replacement of cadmium in Ni–Cd batteries (negative electrode materials) [1–3] since they are cheap and non-polluting. LaNi_5 hydrides have been extensively studied since the discovery of their remarkable hydriding properties by Van Vucht *et al.* [4]. They have a capacity of six hydrogen atoms per formula unit and a desorption pressure of about 2 atm at room temperature. An improvement of LaNi_5 hydrides in electrochemical conditions can be achieved at room temperature by partial substitution of nickel by aluminium, manganese, copper or cobalt; this induces a stabilization of the hydrides without decreasing their hydrogen content [5, 6]. However, for practical applications, the lifetime during charge–discharge cycles must be improved especially in terms of the resistance to corrosion in concentrated KOH solution. The structural [7] and thermodynamic [8] properties of substituted compounds have been described previously. It has been shown that the substitution of nickel by aluminium increases the cell volume and lowers the plateau pressure whilst retaining the LaNi_5 hexagonal structure ($P6/mmm$ space group).

In this paper, we report a structural study of the electrochemical charge–discharge process of deuterium in the $\text{LaNi}_{4.5}\text{Al}_{0.5}$ electrode during an *in situ* neutron diffraction experiment. This was achieved by galvanostatic or potentiostatic monitoring of the deuterium charge during recording of the neutron diffraction patterns. These simultaneous measurements provide information on the phases involved in practical charge–discharge conditions and on the corresponding variations in the unit cell parameters. Differences of behaviour between solid–gas and electrochemical charge processes are also discussed.

2. Experimental details

The intermetallic compound used to prepare the electrode was obtained by melting together the elements in the ratio La:Ni:Al=1:4.5:0.5. Ingots were melted five times in a cooled copper crucible under vacuum in an induction furnace to ensure good homogeneity, and then annealed for 10 days at 900 °C. Metallographic examinations showed that the compound was single phase. Microprobe analysis confirmed the good homogeneity of the material and gave the composition $\text{La}_{1.010(6)}\text{Ni}_{4.50(2)}\text{Al}_{0.48(1)}$. The X-ray diffraction pattern

was indexed in the hexagonal cell ($a = 5.046(2)$ Å, $c = 4.028(4)$ Å, space group $P6/mmm$) in agreement with previous structural investigations [9, 10].

Experiments were carried out in a special silica cell [11–13] developed for a similar study on proton insertion in $\gamma\text{-MnO}_2$. In this cell, given in Fig. 1, the sample (working electrode) is cylindrical. The counterelectrode was made of eight nickel wires of 0.25 mm in diameter regularly spaced around the working electrode to ensure the radial distribution of the current lines and separated from the sample by a silica fibre sheath. The whole sample was exposed to the diffraction beam and the neutrons went through the entire electrode allowing bulk analysis. The composite working electrode was composed of 6.6 g of $\text{LaNi}_{4.5}\text{Al}_{0.5}$ (ground and sifted to a granulometry lower than 36 μm) and mixed with 30 mg of carbon black to ensure good intergranular contact. It was isostatically compressed to 4 kbar in a cylinder (height, 40 mm; diameter, 9 mm) with a nickel wire (diameter, 0.25 mm) in its centre and was placed perpendicular to the diffractometer axis. The electrodes were immersed in KOD (7 N) plus D_2O (isotopic purity, better than 98.5%) as electrolyte and the potential was monitored against a standard Hg/HgO electrode.

Before the *in situ* investigation, a preliminary experiment was performed to set up the electrochemical conditions and to check the electrode behaviour in such a geometry.

The *in situ* neutron diffraction experiment was carried out at room temperature in two stages.

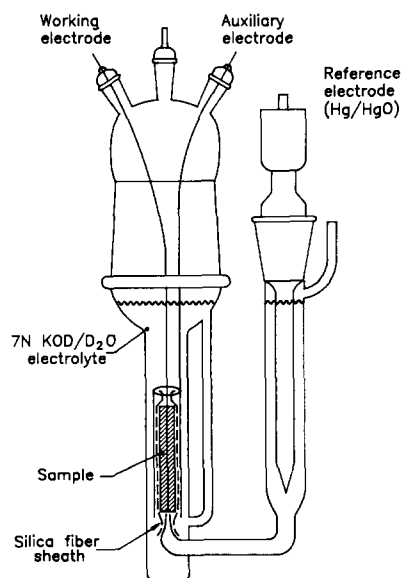


Fig. 1. Schematic diagram of the electrochemical cell assembly. The whole cylindrical sample (working electrode) is in the neutron beam. The mechanical support, not represented here, is made of cadmium shields which screen the beam from the sample in order to limit the background contributions due to silica and electrolyte.

(1) In the first stage of the charge, the electrode was potentiostatically loaded up to 155 mAh (*i.e.* 0.37 H(D) mol⁻¹) to reach the limit of the α phase according to solid–gas absorption data. The deuterium charge was then galvanostatically controlled at two different rates: initially at 50 mA for 10 h and then at 100 mA for 6 h. Each step was followed by relaxation at very low current (1 and 3 h respectively). The process was stopped after a charge of 1265 mAh (*i.e.* 3 H(D) mol⁻¹) before completion of the α to β phase transformation, in order to avoid the disintegration of the electrode which results from the large volume expansion (approximately 20%) occurring during this transition.

(2) Deuterium discharge was then performed under potentiostatic control, by increasing the voltage in steps of 20 mV every 2 h from -1.03 V (which is the equilibrium voltage of the α – β system in this electrolyte) to -0.80 V. The application of the potential step method to remove hydrogen, instead of performing galvanostatic discharge, has two interesting features: firstly, it enables the intensive energy scale to be controlled (*i.e.* the potential is equivalent to the pressure in a solid–gas experiment from a thermodynamic point of view) and, secondly, monitoring of the current on the voltage plateau provides information on the kinetics of the process towards equilibrium. The decrease in the current was recorded during each potential level in order to control the discharge and to determine the exact amount of deuterium removed, which cannot be obtained from crystallographic data at the plateau pressure. Such a determination cannot be performed during the charge which occurs simultaneously with D_2 gas formation at large negative potential. After 5 h open-circuit relaxation, two final steps of 4 h at -0.7 V and -0.5 V were performed to ensure complete discharge of the electrode.

Because the hydriding of $\text{LaNi}_{4.5}\text{Al}_{0.5}$ is an exothermic reaction, we performed an experiment to measure the temperature variations inside the cell. The measurements were made in exactly the same conditions (room temperature, sample, electrochemical environment and charge–discharge rate). The temperature was measured at the surface of the upper part of the electrode with a Cu/Cst thermocouple. Another thermocouple was placed near the reference electrode for comparison. The data show that the temperature variations are less than 1 °C for the whole experiment and this is in agreement with the average dissipated power during the experiment which was estimated to be 10 mW.

Neutron diffraction data were collected on the D1B position-sensitive detector diffractometer at the Institut Laue Langevin (ILL) in Grenoble. The diffractometer was first calibrated with an Al_2O_3 standard sample. Diffraction patterns were recorded every 10 min in the 28–108° range in 2θ with an incident wavelength of

2.5254 Å. The data were analysed using standard ILL programs (ABFFIT [14] and FULLPROF [15]). The fitting procedure used a whole pattern matching program taking into account the nickel lines due to the sample environment and either the α lines when only this phase was present or α and β lines when both phases were observed. This allowed phases to be identified, relative concentrations to be evaluated (from peak intensity measurements) and variations in cell parameters during charge–discharge to be measured. Due to the limited angular range and to the heavy background induced by the sample environment (*i.e.* diffuse scattering peak at $2\theta=55^\circ$), no structural refinements could be obtained from the patterns.

3. Results

During the charging process and after the preliminary deuterium absorption in the α phase, diffraction peaks from the β phase appear whose intensities increase relative to those of the α phase (Fig. 2(a)). A plot of the integrated intensity of the 200 diffraction peak *vs.* time (Fig. 3) provides evidence of the transformation of the α phase into the β phase. It can be seen that the rate of β formation is proportional to the charge current ($C/60$ and $C/30$ respectively (where C/t denotes charge of the full capacity C in t hours)). The phenomenon is less evident for the α phase, but it is worth noting that the integrated intensity of the 200 α line becomes weaker as the charge increases leading to a loss of accuracy in the fitting procedure (which is not the case for the β peak which increases with reaction advancement), and the intensity depends on the proportion of the α phase in the electrode and on the amount of deuterium which enters the solid solution on going from pure intermetallic to oversaturated α phase.

The discharge process was started after a total charge of 1265 mAh had been reacted; the three-dimensional plot presented in Fig. 2(b) shows the decrease in the β peak intensities and the correlated increase in the α peaks. During the potentiostatic discharge, the current (Fig. 4) reaches a maximum after 14 h and then gradually decreases to zero. At the end of the discharge, a small amount of β phase remains visible in the diffraction pattern, although the two final steps at -0.7 V and -0.5 V do not lead to significant current (*i.e.* deuterium release). From the electrochemical data (1265 mAh in charge), the total deuterium content is, at most, 3 deuterium atoms per formula unit if we consider that the reaction yield is 100% without D_2 gas formation. For the discharge, 920 mAh corresponds to 2.17 D mol⁻¹. This result agrees with the observation that the β phase was not completely discharged.

During the whole cycle, a slight but significant variation in the cell parameters is observed for both phases (Figs. 5(a)–5(d)). The a parameter of the α phase increases during charging from 5.045(1) to 5.070(1) Å (+0.50%), whereas c varies from 4.030(1) to 4.035(1) Å (+0.12%). After the low current equilibrium step, these values decrease to 5.067(1) and 4.032(1) Å respectively. For the β phase, the a and c parameters range from 5.320(2) and 4.166(3) Å to 5.345(2) Å (+0.47%) and 4.213(2) Å (+1.10%) respectively. These values are slightly shorter than those expected from previous solid–gas experiments [10] but, in our experiment, the parameters were calculated at the plateau pressure whereas, in the solid–gas process, the values were obtained on a sample charged under 40 bar of hydrogen at room temperature. Since the β cell parameters increase rapidly in the β branch in the solid–gas process, the values must be compared only at a given pressure and temperature. During discharge, the α phase parameters decrease regularly from 5.067(1) to 5.050(1) Å (–0.34%) for a and from 4.032(1) to 4.029(1) Å (–0.07%) for c . The β phase behaves differently: the parameters first decrease to minimum values ($a=5.322(2)$ Å and $c=4.165(3)$ Å) and then increase smoothly to stabilize finally at 5.332(2) and 4.180(2) Å. As mentioned in Section 2 the temperature variations are not significant and these anisotropic variations cannot be related to thermal effects. The phenomenon is of particular interest during the discharge of the β phase since a and c reach minimum when the discharge current is at a maximum (Fig. 4). For both phases, no significant evolution of the width of the diffraction peak is observed and the values remain comparable with the instrumental resolution implying that there is no concentration gradient.

4. Discussion

This *in situ* study of the behaviour of $LaNi_{4.5}Al_{0.5}D_x$ in electrochemical conditions confirms the analogy between electrochemical and solid–gas processes: in both cases, there is an equilibrium between the α and β phases. In the solid–gas process, below the critical temperature T_c , the hydriding reaction leads to an equilibrium between the α and β phases. At the plateau pressure, according to Gibbs phase rule, the two-phase region is monovariant and, for a given temperature, the pressure is independent of the capacity. This involves a progressive transformation of the α into the β phase keeping the cell parameters of the two phases constant. This behaviour has been checked in the solid–gas process for $LaNi_{4.5}Al_{0.5}$ and the isotherm at 25 °C (Fig. 6) exhibits only a single plateau pressure up to 6 H mol⁻¹.

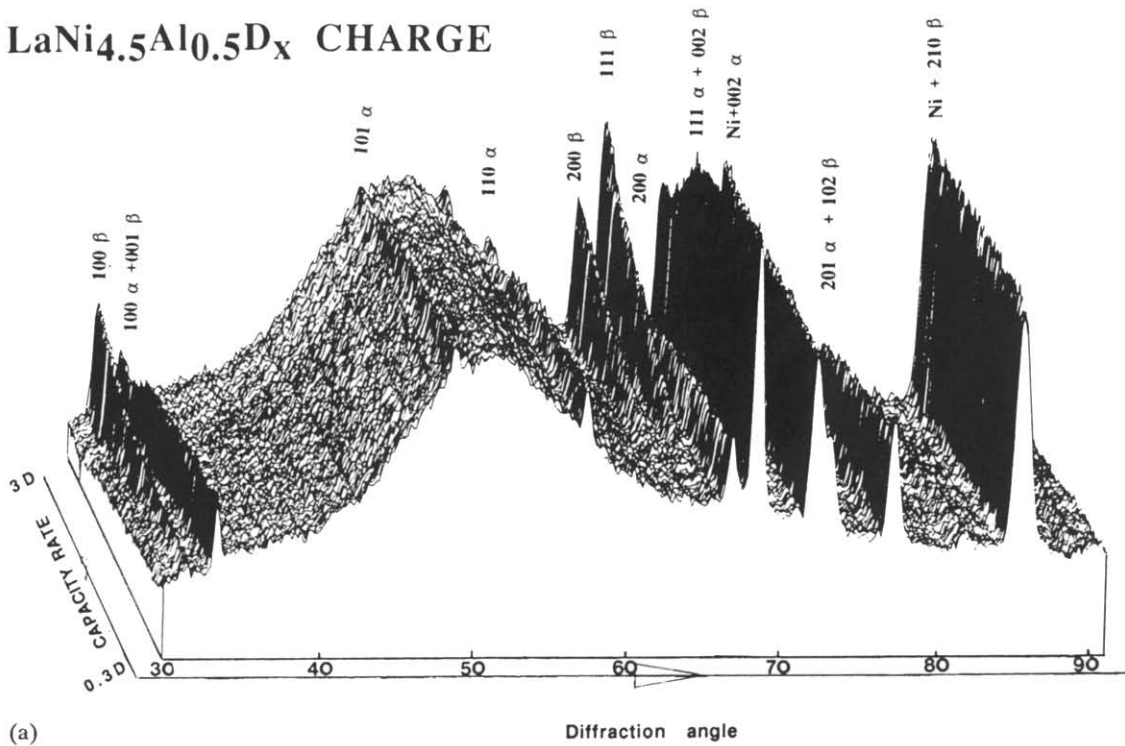
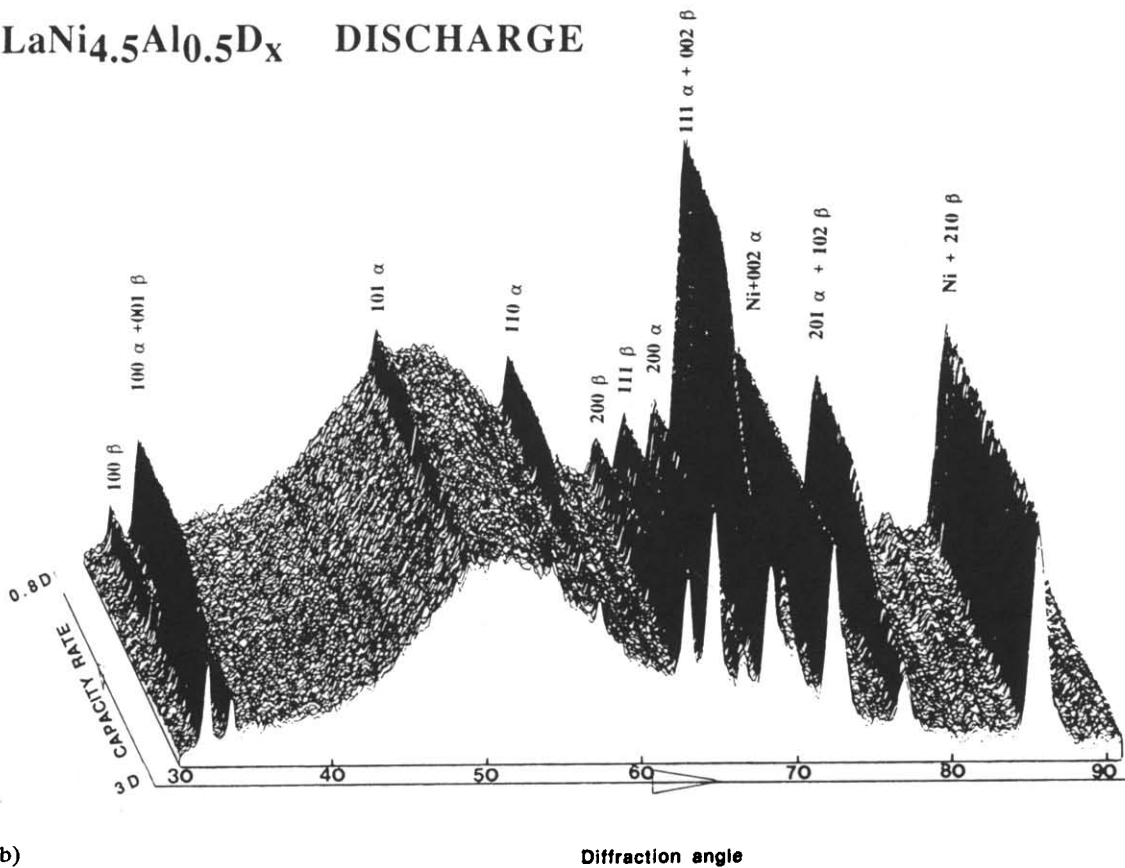
LaNi_{4.5}Al_{0.5}D_x CHARGE**LaNi_{4.5}Al_{0.5}D_x DISCHARGE**

Fig. 2. Evolution of the neutron diffraction patterns during charging (a) and discharging (b). The deuterium atom content is calculated assuming no D_2 gas formation during the charge. The large diffuse scattering peak at $2\theta=55^\circ$ is due to the sample environment (silica cell and electrolyte).

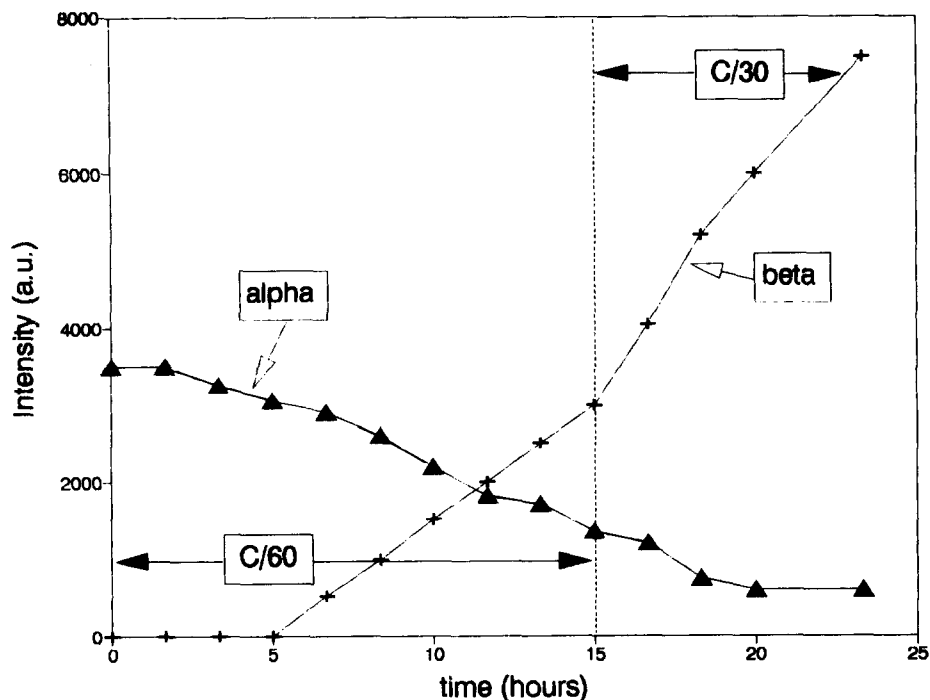


Fig. 3. Evolution of the integrated intensity of the 200 reflection of the α and β phases during charging. Charge rate C/t denotes full capacity C reached in t hours.

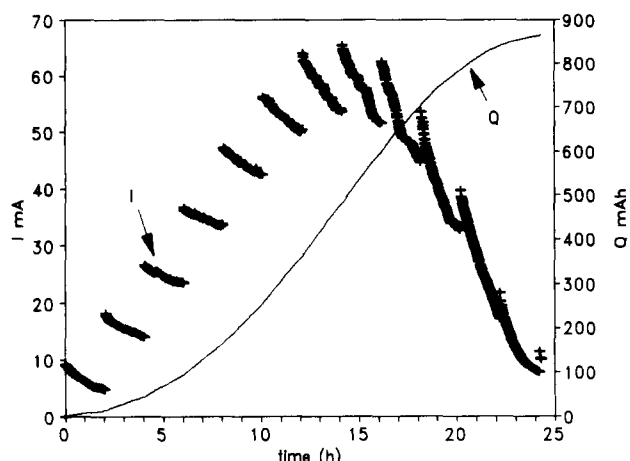


Fig. 4. Variation in the current I vs. time during the -1.03 to -0.8 V (vs. Hg/HgO) multistep discharge procedure and variation in the corresponding charge release Q obtained by integration of the current.

However, in our electrochemical experiment, the analysis of the cell parameters reveals an unexpected evolution of both phases on the equilibrium plateau. The observation that the widths of the diffraction peaks remain constant during the process shows that both phases remain homogeneous even at the grain scale. The main feature of the cell parameter variations is the minimum observed for both a and c parameters during discharge of the β phase at 300–400 mAh closely related to the electrochemical discharge rate, *i.e.* to the maximum current density at that time (Fig. 5(d)).

This behaviour may mean that we can temporarily observe an out-of-equilibrium underconcentrated β phase. This can be explained if we assume that the kinetic rate of the β to α structural transformation is slower than that of the release of hydrogen atoms from the β phase into the α phase under a large potential gradient. After this minimum, the β phase parameters increase and stabilize at a value intermediate between the minimum reached in the electrochemical discharge and that observed at the beginning of the experiment. This shows that a relaxation effect occurs when the reaction is nearly complete. During charging, the parameters of the α phase increase even when the transformation from the α to β phase has started, which indicates that deuterium is still being absorbed into the α lattice. This behaviour can be understood in terms of “dynamic” effects, as the charge-discharge rate does not allow equilibrium to be reached. These results can be compared with those of Ono *et al.* [16] who reported three phases for the $\text{LaNi}_5\text{-H}_2$ system with compositions $x \approx 0.5$ (α phase), $x \approx 3$ (β' phase) and $x \approx 6$ (γ phase) above 80°C . In their experiments, they described an anisotropic lattice expansion where the a axis expansion dominates from α to β' , whereas the c axis expansion is predominant from β' to γ . However, this behaviour has never been reported at room temperature and, moreover, as shown in Fig. 6, the isotherm for $\text{LaNi}_{4.5}\text{Al}_{0.5}$ in the solid-gas process at 25°C exhibits only a single plateau pressure.

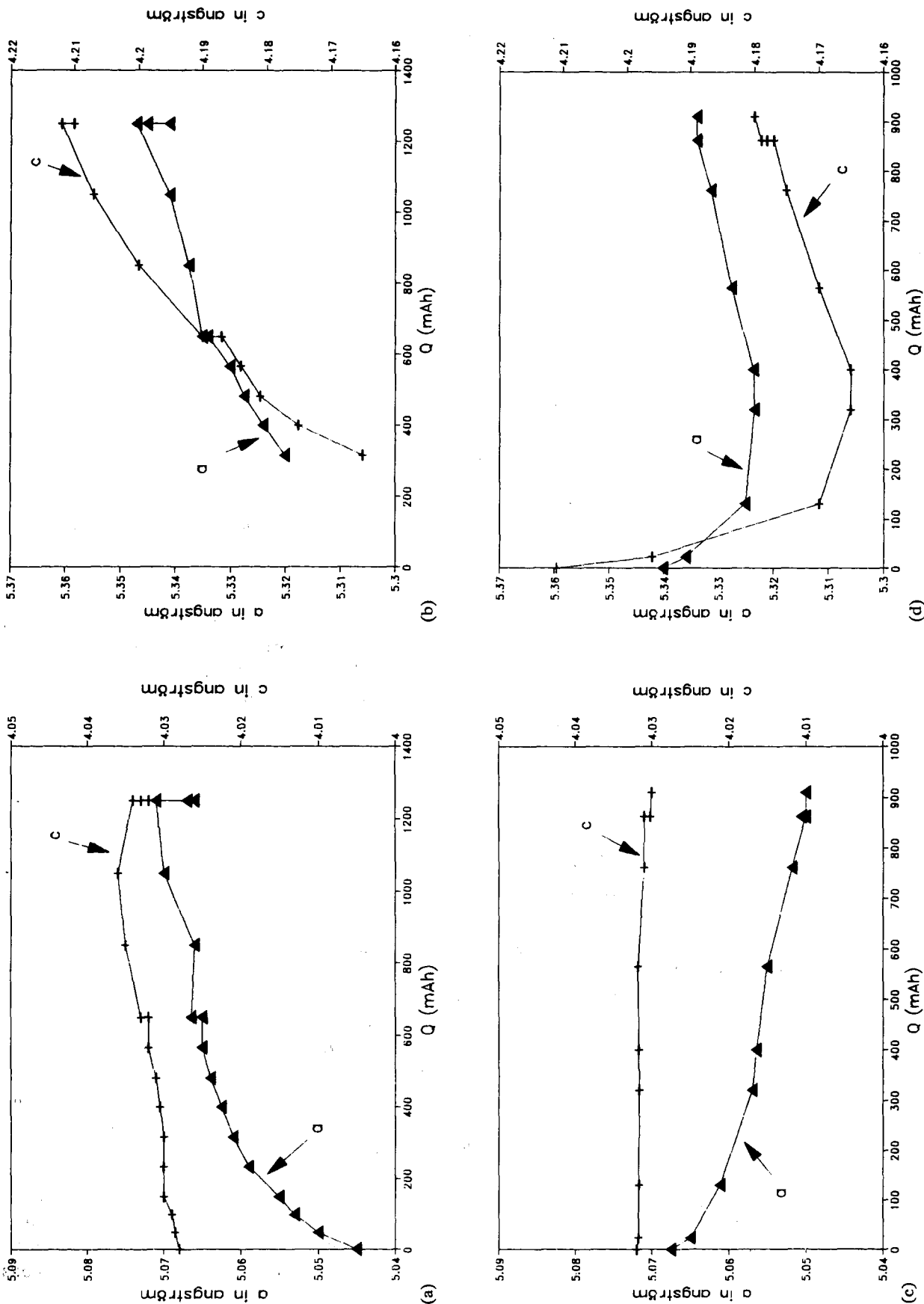


Fig. 5. Variation in the cell parameters of the α and β phases during charge ((a) and (b)) and discharge ((c) and (d)). The main feature is the α and c parameter minima in the discharge process of the β phase when the current is at a maximum (Fig. 4).

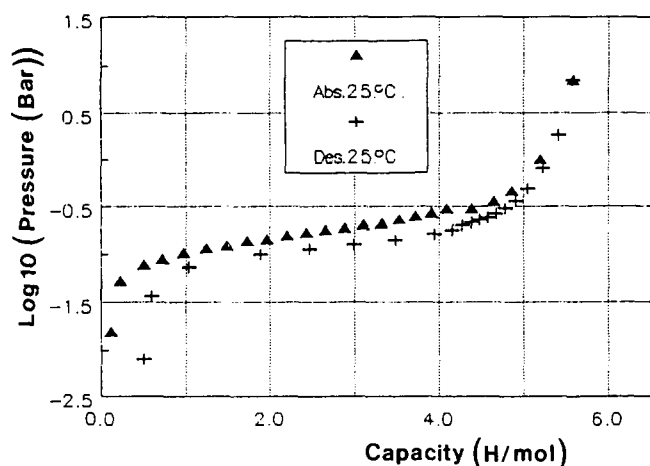


Fig. 6. Isotherm of absorption and desorption of $\text{LaNi}_{4.5}\text{Al}_{0.5}$ at 25°C. Over the whole range of capacity, the curve exhibits only one plateau pressure.

The fact that the β phase cannot be completely discharged may be due to the loss of electrical contact with the current collector for some grains of the composite electrode. This can be attributed to the mechanical effect of the lattice expansion during the charge. This explains the loss of capacity of these materials during electrochemical cycling. Therefore corrosion, which is commonly invoked, may not be the only limiting factor especially at high rates of charge (full capacity charged in 1 h for example).

5. Conclusions

From this investigation, it can be concluded that the structural behaviour of $\text{LaNi}_{4.5}\text{Al}_{0.5}$ during electrochemical charge-discharge is similar to that expected from previous solid-gas studies, but there is evidence of unexpected phases with out-of-equilibrium cell parameters closely related to the discharge rate. The β phase remaining after discharge provides a better understanding of the electrochemical behaviour of the sample under charge-discharge conditions in a geometry very close to that of industrial batteries.

Further experiments are required at various discharge rates in order to obtain a clear understanding of the electrochemical process at the high rates used in com-

mercial batteries. The effect of other substituting atoms such as manganese or cobalt must also be investigated.

Acknowledgments

This research programme was supported by the "Programme Interdisciplinaire de Recherche sur les Sciences pour l'Energie et les Matières Premières" (PIRSEM) from the CNRS.

References

- 1 A. Percheron-Guegan, J. C. Achard, J. Sarradin and G. Bronoel, Electrode material based on lanthanum and nickel. Electrochemical uses of such materials, *French Patent*, 75 16160 (1975), 77 23812 (1977); *US Patent*, 688537 (1978).
- 2 H. Ewe, E. W. Justi and S. Stephan, *Energy Convers.*, 13 (1973) 109-113.
- 3 F. G. Will, Hermetically sealed secondary battery with lanthanum nickel anode, *US Patent*, 3874 928 (1975).
- 4 J. H. N. Van Vucht, F. A. Kuijpers and H. C. A. M. Bruning, *Philips Res. Rep.*, 25 (1970) 25, 133.
- 5 G. Bronoel, J. Sarradin, M. Bonnemay, A. Percheron-Guegan, J. C. Achard and L. Schlapbach, *Int. J. Hydrogen Energy*, 1 (1976) 251.
- 6 H. H. van Mal, K. H. J. Buschow and A. R. Miedema, *J. Less-Common Met.*, 35 (1974) 65-76.
- 7 J. C. Achard, A. J. Dianoux, C. Lartigue, A. Percheron-Guegan and F. Tasset, in G. J. McCarty, H. B. Silver and J. J. Rhyne (eds.), *The Rare Earths in Modern Science and Technology*, Vol. 3, Plenum, New York, 1982, p. 481.
- 8 A. Percheron-Guegan, C. Lartigue and J. C. Achard, *J. Less-Common Met.*, 109 (1985) 287-309.
- 9 A. Percheron-Guegan, C. Lartigue, J. C. Achard, P. Germi and F. Tasset, *J. Less-Common Met.*, 74 (1980) 1-12.
- 10 H. Diaz, A. Percheron-Guegan, J. C. Achard, C. Chatillon and J. C. Mathieu, *Int. J. Hydrogen Energy*, 4 (1979) 445.
- 11 Y. Chabre and C. Poinignon, *ILL Experimental Rep. 5.22.371* Institut Laue Langevin, Grenoble, France, 1990.
- 12 M. Ripert, *Thesis*, Institut National Polytechnique de Grenoble, 1990.
- 13 M. Ripert, J. Pannetier, Y. Chabre and C. Poinignon, *MRS Symp. Proc.*, 210 (1991) 359-365.
- 14 A. Antoniadis, J. Berruyer and A. Filhol, *Acta Crystallogr., Sect. A*, 46 (1990) 692-711.
- 15 J. Rodriguez-Carvajal, *Abstracts of Satellite Meeting on Powder Diffraction*, Congr. Int. Union of Crystallography, Toulouse, France, 1990, p. 127.
- 16 S. Ono, K. Nomura, E. Akiba and H. Uruno, *J. Less-Common Met.*, 113 (1985) 113-117.